EUROPEAN COOPERATION
IN THE FIELD OF SCIENTIFIC
AND TECHNICAL RESEARCH

EURO-COST

IC1004 TD (14)09058
Ferrara, Italy
2014/February/ 5-7

SOURCE: Departement Elektrotechniek TELEMIC,
Katholieke Universiteit Leuven,
Belgium

On the Influence of Meshing on the Accuracy of MoM Solutions for Propagation Applications.

Emmanuel Van Lil, Jan-willem De Bleser
ESAT / TELEMIC
Kasteelpark Arenberg 10 BUS 2444
B-3001 Heverlee
BELGIUM
Phone: + 32-16 321113
Fax: + 32-16 321961
Email: emmanuel.vanlil@esat.kuleuven.be

On the Influence of Meshing on the Accuracy of MoM Solutions for Propagation Applications

Emmanuel Van Lil, Jan-willem De Bleser
Div. ESAT-TELEMIC
KU Leuven
Kasteelpark Arenberg, 10; Bus 2444; B-3001 Heverlee, Belgium
Emmanuel.VanLil@ESAT.KULeuven.Be

***Abstract*—By investigating propagation problems for wind turbines, and more in particular near-field RCS computations, we have noticed that sometimes, even stabilized MoM solutions do not behave as expected. In this paper, we will start with the computation some RCS situations. We found out that discrepancies in some RCS values are due to the choice of the meshing. Usually, standard meshers like gmsh only take into account one object. Unfortunately, to be accurate, all the positions of all objects have to be taken into account, to allow an accurate interaction between the objects. We will go deeper into the fundamentals of the relation between the accuracy and the mesh size and shape for some canonic problems of which the solution is exactly known.**

***Index Terms*—RCS; near-field; wind turbine; mesh size, accuracy MoM solution.**

I. INTRODUCTION

A full wave analysis of near-field RCS computations was performed and compared with other approximations like PO.

The electromagnetic simulation will be detailed (section II), then some examples for simple shapes will be given in view of previously commented simple approximations. (section III). This will inspire us for a discussion on the choice of the meshes to increase accuracy. Conclusions will be drawn in section V.

II. ELECTROMAGNETIC SIMULATION

A low frequency stabilized Moment methods based solution was developed previously [1]. It uses a combined charge and current formulation of which the charge could be eliminated, leading to a very efficient formulation for both dielectric and PEC objects.

$$\begin{bmatrix} E_{inc} \\ H_{inc} \end{bmatrix} = \begin{bmatrix} \dfrac{c_2^2 M_1^r - \kappa c_1^2 M_2^r}{\varepsilon_1 c_1^2 c_2^2} & M_1^c - \dfrac{\varepsilon_2 \kappa M_2^c}{\varepsilon_1} \\ M_1^c - \dfrac{\mu_2 \kappa M_2^c}{\mu_1} & \dfrac{-c_2^2 M_1^r + \kappa c_1^2 M_2^r}{\mu_1 c_1^2 c_2^2} \end{bmatrix} \begin{bmatrix} J_{s,e} \\ J_{s,\mathrm{m}} \end{bmatrix} \quad (1)$$

with $\kappa = M_1^b (M_1^{bT} M_1^b)^{-1} M_1^{bT}$

Note that both normal and tangential components of the incident field can be used, leading to a high accuracy. For the case of a sphere, of course, the analytical solution exists as a series of spherical orthogonal functions and was found by Mie [2]. In Fig. 1 we can indeed see that the accuracy of the combined charge and current formulation is best, even in the monostatic case the difference is very small.

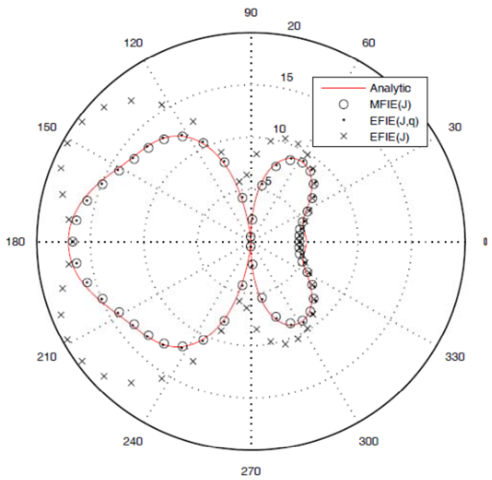

Fig. 1: RCS computations for an r=λ/2 PEC sphere with 3 kinds of integral equation implementations.

One should also notice that in the limit case for small spheres the monostatic RCS is proportional to $9\pi a^2(ka)^4$, while a PO computation would give us the result 64/9 or 7.111 $\pi a^2(ka)^4$, which is found on many web sites, even if the slope of the curve is similar. We should not wonder about this difference, since PO is only valid for surfaces that are nearly flat, which is not the case for a small sphere. The PO completely fails for a large sphere as can be seen in Fig. 2. Another PO approximation, using only the illuminated part of the sphere, obviously collapses for small spheres, since this assumption is only valid is the sphere is much larger that the wavelength.

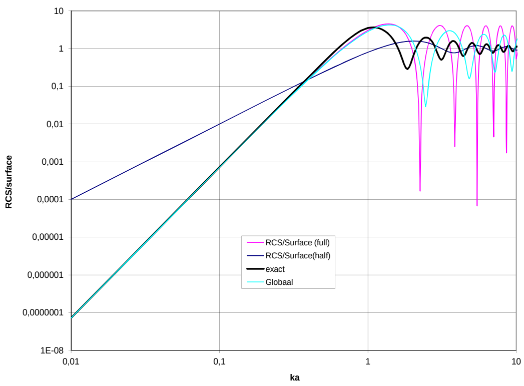

Fig. 2: PO RCS computations for a PEC sphere in function of its size and the exact value.

For RCS computations at one frequency and different distances, we can easily solve (1) with many incident fields, corresponding with the different distances from the source to the object, making the solution even more efficient, since the matrices in the right hand side remain the same.

III. EXAMPLES

A figure for the monostatic RCS of a finite PEC cylinder with dimensions of 10 m in height and 1 m radius is shown for a wavelength of 1 m in Fig. 3. The polarization of the transmitting dipole is parallel with the axis of the cylinder.

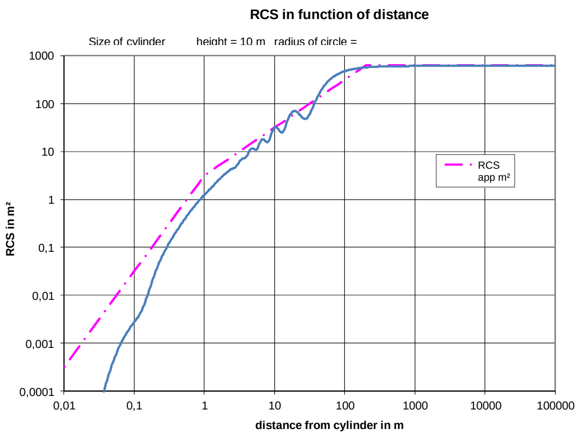

Fig. 3: Normalized monostatic near-field RCS of a PEC cylinder with a proportion h/r=5 and r=λ in function of the distance to the specular reflection point.

We had already shown the linear approximation for the cylinder in [3], represented here in the dash-dotted line. Now we can see that only in a few points this value is exceed by up to 66% or 2 dB. The far-field value of $2\pi rh^2 / \lambda$ or in this case 200 π is well followed after the last breakpoint at 200 m. Below the first breakpoint at 1 m, the approximation is not so well followed, but the approximation is always larger than the (already very small) real RCS. Also, this distance is more of academic value, since in practice no radar or target should be so close to the interfering object. We note however a relatively large relative error when the transmitter is very close to the object. This is indeed a difficult problem to solve. As we have previously experienced in the case of PO, the mesh should be adapted to the presence of the source and cannot be considered alone any more. Here the mesh was chosen constant throughout all computations at all distances. It has 4628 triangular elements (and 2316 nodes corner points) and is shown in Fig. 4.

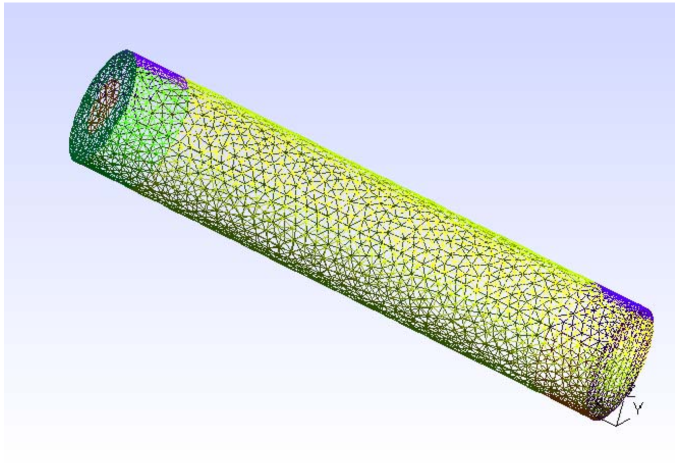

Fig. 4: Mesh used for the computations of the RCS.

This will force us to discuss the influence of the meshing both for expansion as for testing functions.

IV. ACCURACY CONSIDERATIONS

We have already shown that using a combination of tangential and normal boundary conditions was increasing the accuracy [3]. This forced us to end up with non-square MoM matrices. We will now prove for a simple case that this is not at all an inefficient idea. We will even simplify the problem further, and consider the case of a static 2D strip, already solved by Maxwell over 100 years ago. We first consider the case where the number of (pulse) expansion function is equal to the number of testing functions (point matching). The normalized charge distribution is shown in Fig. 5.

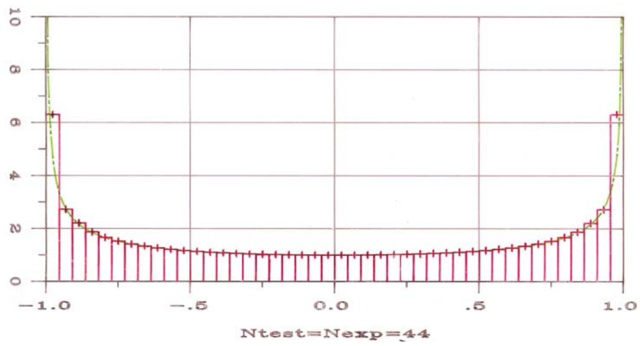

Fig. 5: Normalized charge distribution on a static strip (center charge =1 C/m², 44 equally spaced test and expansion functions).

It is obvious that, when we increase the number of test and expansion functions, the accuracy with which the exact distribution (becoming infinite at the edge of the strip) is followed increases (Fig. 6 for N=1250).

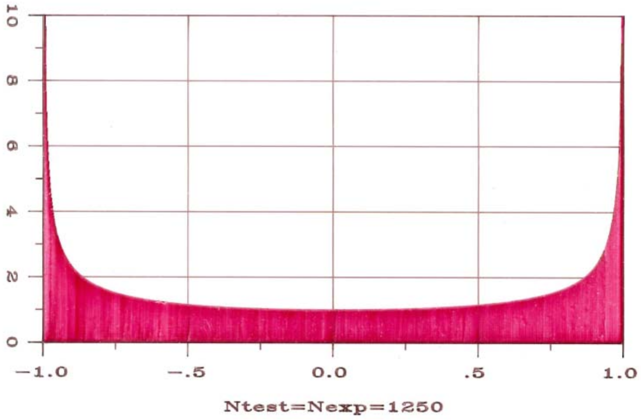

Fig. 6: Charge distribution on a static strip (center charge = 1 C/m², 1250 equally spaced test and expansion functions; the exact solution (green dash-dotted line) is barely visible).

Since the matrix is in this case Toeplitz very efficient algorithms exist to do so. The computational effort only increases with N^2, while the matrix only require N memory positions. Of course many accuracies can be defined. If one considers the edge function, the absolute error becomes larger and larger. The error near the center of the strip becomes smaller and smaller. We will consider here a global value, like the capacitance of the strip (this can be compared with the global RCS for the problem at hand). It is obvious that the error continuously decreases when the number of functions (or mesh elements) increase (Fig. 7). The rate of the relative accuracy is approximately $1/N^2$.

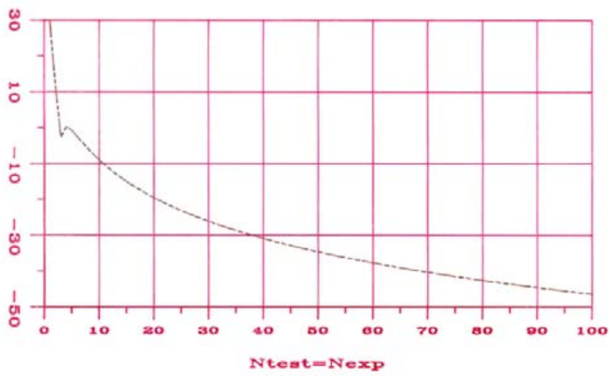

Fig. 7: Relative error on the capacitance in function of the number of equally spaced functions (logarithmic scale; 0 = 1%, -20 = 0.1%).

It is also obvious, that, if we increase the resolution of the mesh where the variable to be solved (in this case the charge density) varies the most, we will obtain a much better result with much less functions. For the strip case, the obvious choices are the zeroes of Chebyshev polynomials. The charge density with unequally spaced distributions is shown in Fig. 8.

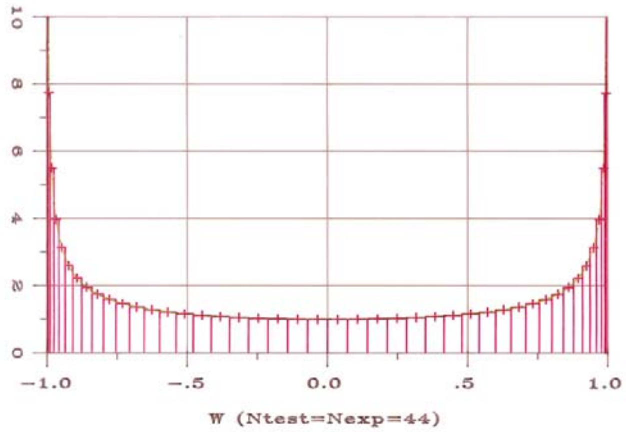

Fig. 8: Charge distribution on a static strip (center charge =1 C/m², 44 unequally spaced test and expansion functions).

We can see that the capacitance error is now decreasing much more rapidly in function of the number of functions (Fig. 9). The decrease rate still remains $1/N^2$, but we will reach a high accuracy much faster. It should also be noted that the computational effort is now increased to N^3, since the matrix has no special features like Toeplitz, but this is a special case for geometries with a lot of symmetries that do not occur very often in practice.

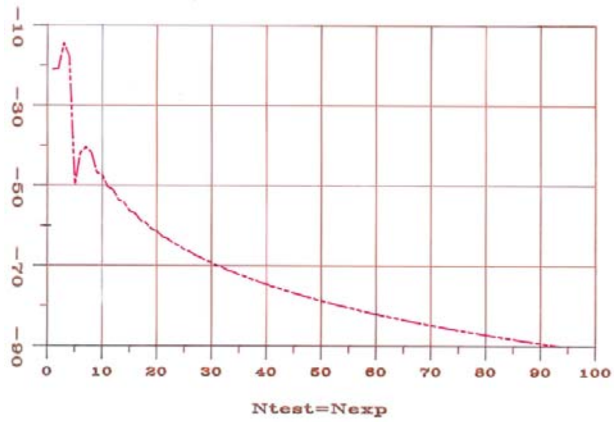

Fig. 9: Relative error on the capacitance in function of the number of unequally spaced functions (logarithmic scale; 0 = 1%, -20 = 0.1%).

Finally, we can investigate the case of a different (larger) number of testing functions with respect to the number of expansion functions. One example of a charge distribution with 9 expansion functions and 14 testing functions is given in Fig. 10. If we take less (13) testing functions, we notice that the testing functions stays just outside the expansion functions close to the edges of the strip (Fig. 11).

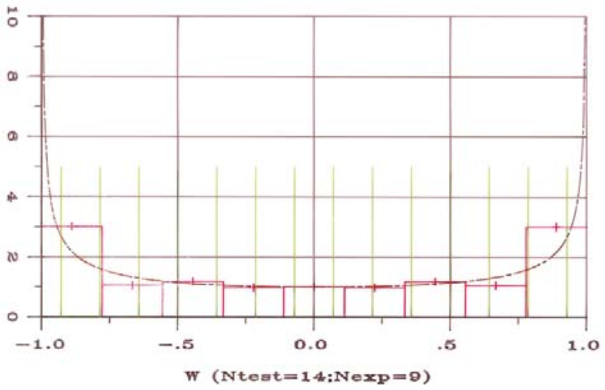

Fig. 10: Charge distribution on a static strip (center charge =1 C/m², 9 equally spaced expansion and 14 equally spaced test functions (green Dirac impulses); exact solution = dark dash-dotted line).

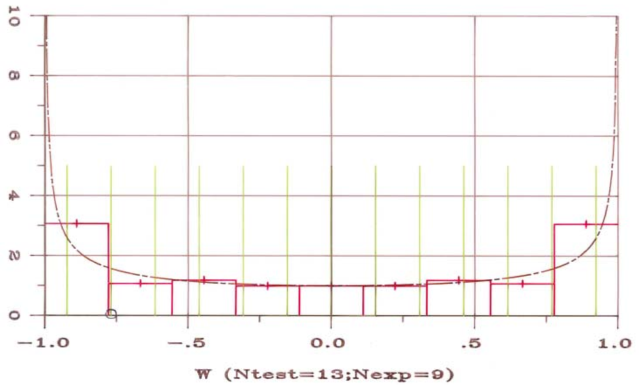

Fig. 11: Charge distribution on a static strip (center charge =1 C/m², 9 equally spaced expansion and 13 equally spaced test functions (green Dirac impulses); the exact solution is shown in dark dash-dotted line).

This choice will have its influence on the accuracy. It will be clearly visible on the accuracy of the charge in the central expansion function. Indeed, in the 14 test function case, the extreme expansions function as well as the central one are tested twice, leading to a lower accuracy than in the 13 test function case (Fig. 12).

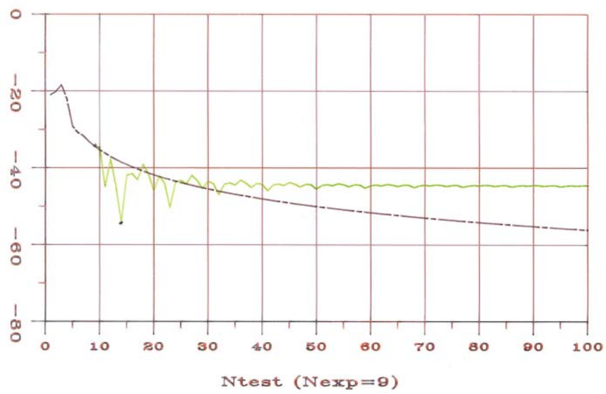

Fig. 12: Relative error on the central charge distribution in function of the number of equally spaced testing functions (logarithmic scale; -40 = 1%, -60 = 0.1%; the number of expansion functions is 9).

However, on a global value like the capacitance, this influence is not so drastic. Indeed, we can see, that the accuracy increases, as long as we do not make the matrix too rectangular (Fig. 13). A further increase does not improve the accuracy.

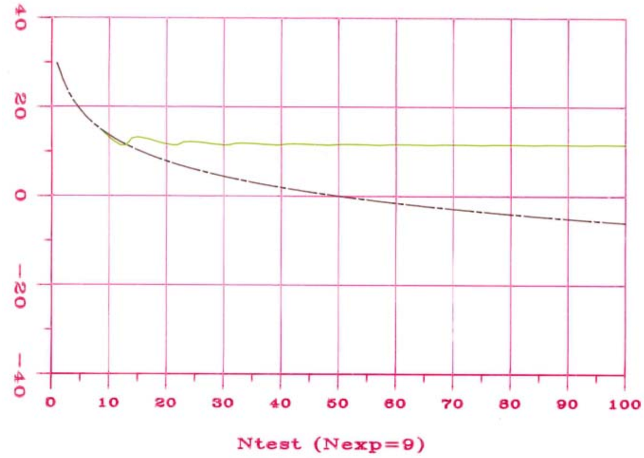

Fig. 13: Relative error on the capacitance in function of the number of equally spaced testing functions (logarithmic scale; 20 = 1%, 0 = 0.01%; the number of expansion functions is 9).

Finally, we can see, that the accuracy increases also on a global value like the capacitance, as long as we do not make the matrix too rectangular (Fig. 13). A further increase does not improve the accuracy just as in the case of the accuracy of the central element.

The advantage of this procedure is that the computational time only increases linearly with the number of extra testing functions. This is performed on an old HP-1000 computer in with a real-time operating system (RTE6) (Fig. 14).

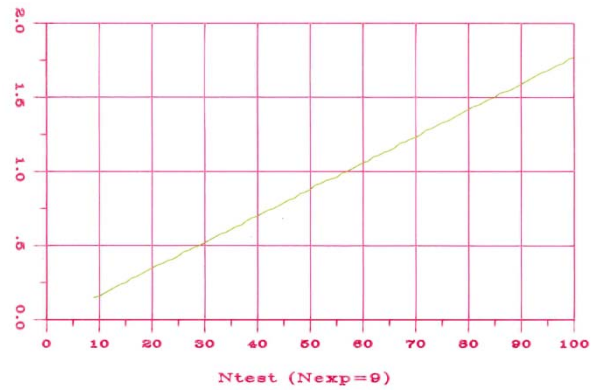

Fig. 14: Cpu time in functions of the number of test functions (9 expansion functions).

V. CONCLUSIONS

The computation of the near-field RCS of a finite cylindrical tower (inspired by a windmill [4]) has lead us to discuss the accuracy of full-wave solution moment methods now from the viewpoint of the choice of expansion and test functions and according mesh densities.

REFERENCES

[1] Jan-willem De Bleser, Emmanuel H. Van Lil and Antoine R. Van de Capelle, “Split Formulation of the Charge and Current Integral Equations for Arbitrarily-Shaped Dielectrics”, IEEE trans. Antennas and Propagat., Vol. AP−61, No. 1, pp. 302−310, January 2014

[2] G. Mie, “Beiträge zur Optik Truber Medien Speziell Kolloidaler Metallösungen”, Annalen der Physik, vol. 25, pp. 377–445, 1908.

[3] Jan-willem De Bleser, Emmanuel Van Lil and Antoine Van de Capelle, "A comparison of implementations of a combined charge and current formulation of the method of moments", URSI General Assembly and Scientific Symposium, pp. 1-4, Istanbul, Turkey, 13-20 August 2011

[4] Emmanuel H. Van Lil, Jan-willem De Bleser and Antoine R. Van de Capelle, " Computations of the Effects of Wind Turbines in the close near field of RF Installations", EUCAP 2011, pp. 1-5, Rome, 11-15 April 2011